Journal of Alloys and Compounds 705 (2017) 309–313

Contents lists available at ScienceDirect

Journal of Alloys and Compounds

journal homepage: http://www.elsevier.com/locate/jalcom

Microwave absorbing properties of FeCrMoNiPBCSi amorphous powders composite

Shuwen Chen [a, b], Guoguo Tan [a, b], Xisheng Gu [a, b, c], Qikui Man [a, b, *], Fashen Li [a, b], Chuntao Chang [a, b, **], Xinmin Wang [a, b], Run-Wei Li [a, b]

[a] Key Laboratory of Magnetic Materials and Devices, Ningbo Institute of Materials Technology & Engineering, Chinese Academy of Sciences, Ningbo, Zhejiang 315201, China
[b] Zhejiang Province Key Laboratory of Magnetic Materials and Application Technology, Ningbo Institute of Materials Technology & Engineering, Chinese Academy of Sciences, Ningbo, Zhejiang 315201, China
[c] Research Center of Magnetic and Electronic Materials, College of Materials Science and Engineering, Zhejiang University of Technology, Hangzhou 310014, China

ARTICLE INFO

Article history:
Received 27 October 2016
Received in revised form
18 January 2017
Accepted 10 February 2017
Available online 11 February 2017

Keywords:
Fe-based amorphous
Spherical powder
Electromagnetic property
Electromagnetic microwave absorbing

ABSTRACT

The FeCrMoNiPBCSi amorphous alloy system with good soft-magnetic property and high glass forming ability was utilized to prepare amorphous powders which are integrated for electromagnetic wave absorbing composite with silicone-matrix. The absorption parameters were measured by tuning the sample thickness and volume fraction strictly. The results show that FeCrMoNiPBCSi amorphous alloy system is more prone to attain impedance matching and has strong ability on electromagnetic wave attenuation. The value of reflection loss reaches −60.3 dB at 7.08 GHz for the composite (30 vol % powders) and the bandwidth reaches 2.30 GHz for RL < -10 dB.

1. Introduction

As electronic equipment has been widely used for military and civil applications such as microwave interference protection and microwave darkness [1,2], the microwave devices develop to be high frequency, integration and functionalization, as well as the electronic component to be surface installated. The electromagnetic(EM) wave energy grows at the rate by 7–14% per year [3], bringing out serious damages for information security and human health. Thus the demands for EM shielding material and absorbing material applied for electronic devices are rapidly sharpening [4,5].

Compared with amorphous powders, common absorber such as crystalline metal powders [6] are restricted to lower resistivity and poorer corrosion, while ferrites [7] are deficient for higher temperature resistance and saturation magnetization. Besides, amorphous powder possesses the disorder atomic structure which is not only beneficial to reduce eddy current loss but also expand the skin depth for GHz frequency application. This is the reason why amorphous alloy with lower complex permittivity easily reach well impedance matching [8,9]. Consequently, the amorphous-filler composite is expected as a promising candidate for absorption application.

Recently, special attentions have been focused on glass-coated amorphous microwires attributed to their prominent electromagnetic performance for absorbing material and electromagnetic shielding application on high-frequency and broadband absorption [10–14]. However, owing to lower glass forming ability and complicated preparation, the research on amorphous soft-magnetic powder application at higher frequency is rarely reported.

In this work, FeCrMoNiPBCSi amorphous powder with excellent corrosion, wear resistance and soft-magnetic property prepared by gas atomization technique was selected as the magnetic absorber. As a nonmagnetic hydrocarbon, the silicone has merits of low permittivity, feasible processability and rapid prototyping, making

* Corresponding author. No. 1219 Zhongguan West Road, Zhenhai District, Ningbo, Zhejiang 315201, China.
** Corresponding author. No. 1219 Zhongguan West Road, Zhenhai District, Ningbo, Zhejiang 315201, China.
E-mail addresses: manqk@nimte.ac.cn (Q. Man), ctchang@nimte.ac.cn (C. Chang).

http://dx.doi.org/10.1016/j.jallcom.2017.02.089
0925-8388/

it be an appropriate matrix to play an important role in tuning EM parameters. The EM parameters tested from 0.1 to 18 GHz are investigated to explore desirable absorption materials. The results demonstrate that amorphous absorber has strong EM wave attenuation abilities for GHz frequency absorption.

2. Experimental

$Fe_{63}Cr_8Mo_{3.5}Ni_5P_{10}B_4C_4Si_{2.5}$ (at.%) alloy ingots were fabricated by vacuum induction melting furnace of a mixture of industrial raw material. Once the vacuum was below 10^{-3} Pa by utilizing gas atomization device, the ingots were re-melted and atomized into powders by high-pressure nitrogen. The acquired fine powders above 600 mesh (the diameter~23 μm) were sieved out for amorphous-filler composite. The phase compositions and microstructures of the obtained powders were detected by X-ray diffraction (XRD, Bruker AXS) with CuKa and scanning electron microscopy(SEM, Hitachi S-4800), respectively. The saturation magnetization and coercivity were measured by means of vibrating sample magnetometer (VSM, Lakeshore 7304, USA) at an applied field of 10 kOe. Prior to mixed with silicone, various volume concentration magnetic powders (10 vol%, 20 vol%, 30 vol%, 35 vol%, 40 vol%, 50 vol%) were coated with coupling agent on their surfaces to elevate oxidation resistance and dispersed in acetone solution. Ultimately, the composite samples were molded into a toroidal shape with inner and outer diameter being 3.04 mm and 7.00 mm, respectively. The complex permeability ($\mu = \mu' - j\mu''$) and permittivity ($\varepsilon = \varepsilon' - j\varepsilon''$) of annular samples were tested by coaxial waveguide method using vector network analyzer (Agilent N5234A) from 0.1 to 18 GHz.

3. Results and discussion

Fig. 1 presents both surface morphology and XRD spectrum of amorphous powders. No obvious defect on the surface of single powder particle was observed which may result in multiple scattering and interface polarization, thereby influencing the microwave absorbing parameters. The particles appear mostly spherical or ellipsoidal with the diameter less than 20 μm. XRD pattern reveals there is no remarkable crystallization peak, indicating that the powder is of fully amorphous structure and the alloy system has high glass forming ability.

The static hysteresis loop of $Fe_{63}Cr_8Mo_{3.5}Ni_5P_{10}B_4C_4Si_{2.5}$ amorphous soft-magnetic powders was measured at room temperature. As observed in Fig. 2, due to the completely amorphous structure for isotropic intrinsic feature, the coercivity (H_c) reduced to 1.3 Oe coupling with the saturation magnetization (M_s) for 47.5 emu/g.

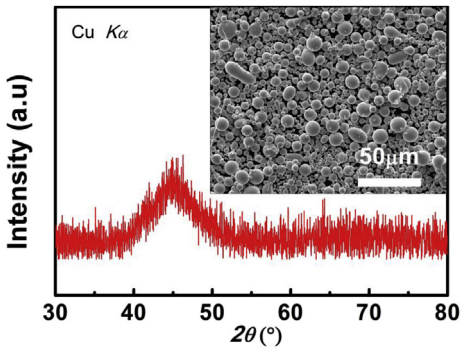

Fig. 1. XRD pattern of $Fe_{63}Cr_8Mo_{3.5}Ni_5P_{10}B_4C_4Si_{2.5}$ amorphous powders obtained by gas atomization method, SEM image of above powders surface morphology is in the inset.

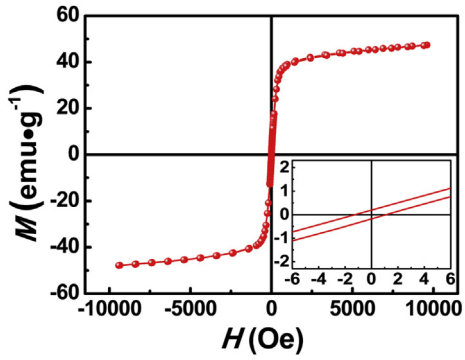

Fig. 2. Static hysteresis loop of $Fe_{63}Cr_8Mo_{3.5}Ni_5P_{10}B_4C_4Si_{2.5}$ amorphous soft-magnetic powders.

What's more, the disorder atomic structure makes the amorphous powder provided with electrical resistivity ($\rho \geq 120\ \mu\Omega$ cm [15–17]) many times greater than those of metallic alloy powder, thus allowing for GHz range operation and lower energy dissipation.

In view of the microwave absorption ascribed for dielectric loss and magnetic loss, it is important to well balance permeability and permittivity for improving absorption performance. The acquired EM parameters for silicone-matrix composites filled with various volume fractions of amorphous powders at 0.1–18 GHz are illustrated in Figs. 3 and 4. As results of eddy current loss and ferromagnetic resonance, the real permeability (μ') gradually decreases as the frequency increases, yet increases as the filler volume concentration increases. Meanwhile, the imagine permeability (μ'') of the composites represents similar trend as μ', although the resonance frequency at which the μ'' has a maximum value shifts to lower with a increasing volume content. According to Fig. 4, it is clear that real permittivity (ε') is almost independent of frequency over whole range 0.1–18 GHz, due to weaker interfacial polarization compared with the flake-like or the wire-like. Besides, imagine permittivity (ε'') seems to be an approximate constant with amounts of small fluctuant peaks originating from the measuring deviation. So the dynamic variation of μ'' (imagine part of the permeability) with frequency is one of the main factors that affect the EM loss.

Fig. 5 illustrates the experimental and calculated reflection loss curves of 40 vol% composite with thickness of 2.5 mm. The experimental result was measured in the coaxial short-circuited line similarly done by Zhuravlev [18]. The frequency of absorption peak deviates from 9.8 GHz (experimental) to 9.1 GHz (calculated). Besides, the calculated absorption frequency band for RL < −10 dB becomes narrow as compared with the experimental.

According to Transmission Line Theory, for a single-layer absorbing material with a metal plate, the input impedance is:

$$Z_{in} = Z_0\sqrt{\mu_r/\varepsilon_r}\tanh\left(j(2\pi ft/c)\sqrt{\mu_r\varepsilon_r}\right) \quad (1)$$

$$Z_0 = \sqrt{\mu_0/\varepsilon_0} \quad (2)$$

Where Z_0 (377 Ω) is the characteristic impedance of free space, μ_r is the complex permeability, ε_r is the complex permittivity, f is the frequency of incident EM wave, t is the thickness of absorbing sample, c is the velocity of light in free space. When an EM wave is incident on absorbed sample layer, the EM wave reflection loss can be calculated according to the values of Z_0 and Z_{in} using the measured complex permeability and complex permittivity at given frequencies [19]:

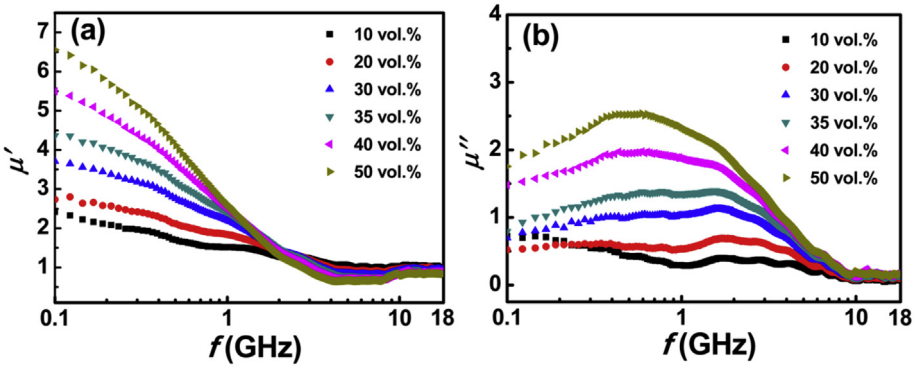

Fig. 3. The frequency dependence of (a) real permeability, and (b) imagine permeability for the FeCrMoNiPBCSi amorphous powders/silicone composites with various volume concentrations.

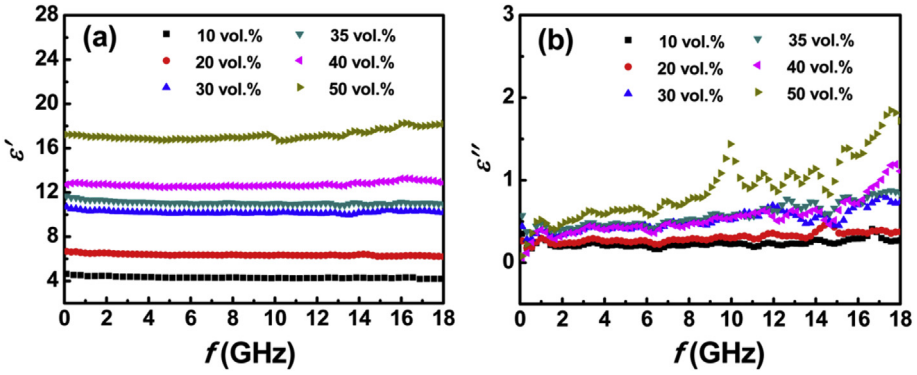

Fig. 4. The frequency dependence of (a) real permittivity, and (b) imagine permittivity for the FeCrMoNiPBCSi amorphous powders/silicone composites with various volume concentrations.

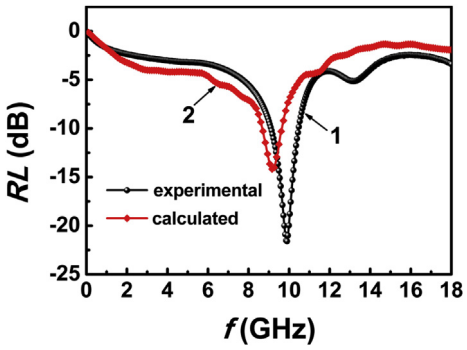

Fig. 5. The frequency dependence of reflection loss for 40 vol% composite at thickness of 2.5 mm Curve1: the experimental result. Curve 2: the calculated result.

$$RL = -20\log\left|\frac{Z_{in}-Z_0}{Z_{in}+Z_0}\right| \tag{3}$$

The interface reflection model [19] explains that the value of reflection loss absorption peak frequency f_m is related to absorbed layer thickness t_m as following formula:

$$t_m = \frac{n}{4}\frac{c}{f_m\sqrt{|\mu_r\varepsilon_r|}},\ n = 1,\ 3,\ 5\ \ldots \tag{4}$$

This denominates the quarter-wavelength matching model [20–22]. Here, only matching thicknesses $t = \lambda_g/4$ and $t = 3\lambda_g/4$ are considered, where $\lambda_g = \lambda/(\mu\varepsilon)^{1/2}$, λ and λ_g represent the wavelength in the free space and the medium, respectively, other higher order wavelength matching are ignored. Combined with interface reflection model, Eqs. (1) and (3), both perfect matching parameters and finite matching parameters were calculated. Based on the above formulas, we can conclude that the matching thickness (t_m) and matching frequency (f_m) are essentially controlled by the value of $|\mu_r\varepsilon_r|$. To achieve optimal reflectivity, $\sqrt{\mu_r/\varepsilon_r}$ should be close to unity for the impedance matching between materials and free space [23].

It is well known that both the impedance matching and intrinsic EM loss determine the incident microwave with minimum reflection and maximum transmitted attenuation for the metal-backed single layer absorber. To make full use of reflection reduction, as much as possible microwaves are required to enter into the structure to be dissipated into heat through the mechanism of dielectric loss and magnetic loss and seldom is reflected to free space. On the other hand, the normalized input impedance with respect to the free space (Z_{in}/Z_0) should be 1 for no reflection.

3.1. Perfect matching parameters

Perfect matching parameters are directly carried out with following intrinsic parameters: μ', μ'', ε', ε'', f_m and t_m. The reflection loss is determined by integrating Eq. (1) with Eq. (3) and derived from efficient matching of above parameters. In this condition, at the perfect matching point, the phases of reflective EM waves from absorbing anterior interface and metal plate back interface are out of 180° and the intensity of two reflected waves is equivalent, then there is no reflective wave out of the absorbing material. Table 1

Table 1
Absorption properties of $Fe_{63}Cr_8Mo_{3.5}Ni_5P_{10}B_4C_4Si_{2.5}$ amorphous soft-magnetic powders composite under perfect matching absorbing condition (only $\lambda_g/4$ is considered).

V_c (vol%)	f_m (GHz)	t_m (mm)	$\lvert Z_{in}/Z_0\rvert$	RL (dB)	Δf (GHz) (RL < −10 dB)	Δf (GHz) (RL < −20 dB)
10	4.15	8.20	1.940	−9.7	0	0
20	4.15	6.64	1.080	−23.1	2.19	0.60
30	7.08	3.55	0.996	−60.3	2.30	0.63
35	8.07	3.14	0.999	−55.3	2.30	0.81
40	8.33	2.92	0.994	−54.1	1.86	0.40
50	10.4	1.94	0.994	−50.8	1.72	0.85

lists the absorbing parameters of composites which are under perfect matching conditions (only at matching thicknesses $t = \lambda_g/4$). It is notable all the composites obtain excellent absorption performance except for the 10 vol% composite whose ratio of $|Z_{in}/Z_0|$ is much large than 1. The matching thickness t_m (at which the absorbing material has a minimum of return loss) far exceed 5 mm, which is too thick for practical application. The calculated corresponding frequency dependence of reflection loss curves are illustrated in Fig. 6. The RL peak position shifts to higher frequency as the increasing volume fraction for ferromagnetic powders. For the content of 10 vol% and 20 vol%, the characteristics of dual absorption peaks give rise to a effective broadening for absorption bandwidth. The matching frequency for the second RL peak is in accordance with the three-quarter wavelength.

Adding 30 vol% filler makes it possess an optimal reflection loss of −60.3 dB at 7.08 GHz at a perfect matching thickness of 3.55 mm, when the $|Z_{in}/Z_0|$ equals 0.996. Moreover, the absorption frequency bandwidth reaches 2.30 GHz for RL < −10 dB and 0.63 GHz for RL < −20 dB, respectively. When volume concentration varies from 35 to 50 vol%, the composite has excellent absorbing property for 8–12 GHz at thickness <3.14 mm. Thus this absorbing material has potential X-band application.

3.2. Finite matching parameters

In general, the amplitude of RL is difficult to reach minimum reflectivity when $|Z_{in}/Z_0|$ is away from 1. However, there is still a minimum value at a certain thickness. In this case, it is called the finite matching compared to the perfect matching [24,25]. The finite matching parameters which demonstrate the frequency dependence of RL for samples with a thickness of 1.8 mm are shown in Fig. 7. The RL absorption peak moves to lower frequency as the increasing volume fraction, which is consistent as the Bruggeman equation indicated [26]. As shown, RL < −10 dB can be achieved for volume concentration ranging from 30 vol% to 50 vol%, moreover the minimum RL is −30.9 dB at 9.80 GHz for the 50 vol% filler composite and the absorption frequency bandwidth becomes

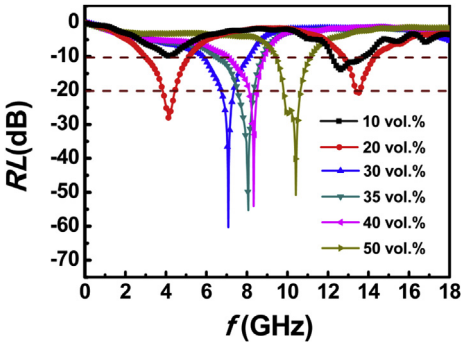

Fig. 6. The frequency dependence of reflection loss for various volume fraction composites under perfect matching absorbing condition.

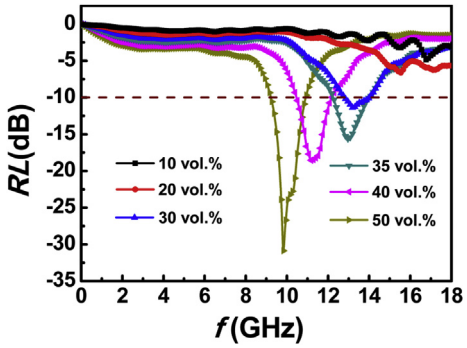

Fig. 7. The frequency dependence of reflection loss for various volume fraction composites with a thickness of 1.8 mm.

1.73 GHz for RL < −10 dB.

Fig. 8(a) illustrates the RL curves for the 30 vol% filler composite with various thicknesses (1.0–5.0 mm). No obvious EM absorption peak appears when the thickness is smaller than a certain value. Meanwhile, the RL peak position shifts to lower frequency with the increasing sample thickness, which can be explained by Eq. (4) resulting from an inverse relation between t_m and f_m in quarter-wavelength matching model. Surprisingly, dual-frequency absorption peaks can be found at a thickness of 5.0 mm, the reflection loss for the first peak is −14.3 dB at 4.70 GHz for C-band region, and the second is −19.2 dB at 14.72 GHz for K_u-band region, as well as the corresponding frequency bandwidth for RL < −10 dB reaches 2.7 GHz and 1.2 GHz, respectively. Combined with Eq. (4), Fig. 8(b) shows the dependence of thickness ($\lambda_g/4$ and $3\lambda_g/4$) on entirely measured frequency, the conceivable reason is that when the sample thickness exceeds 4.01 mm which simultaneously satisfies $\lambda_g/4$ and $3\lambda_g/4$ in the medium(4.70 GHz peak corresponds to $n = 1$ and 14.72 GHz peak corresponds to $n = 3$), dual absorption peaks will appear. At a thickness of either $\lambda_g/4$ or $3\lambda_g/4$, the incident and

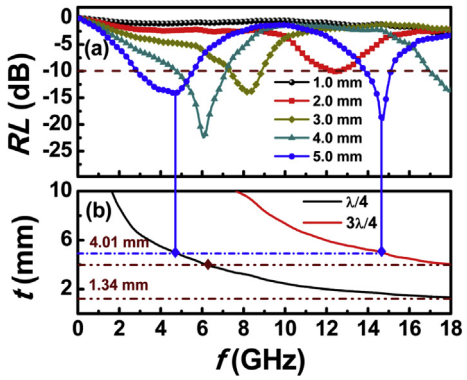

Fig. 8. The dependence of RL on frequency with different thicknesses (a) and the dependence of thickness (λ/4 and 3λ/4) on frequency (b) for 30 vol% filler concentration composite.

reflected waves in the material are out of phase by 180°. When the sample is thinner than 1.34 mm, there is no absorption peak. In addition, sole absorption peak can be obtained with the thickness ranging from 1.34 mm to 4.01 mm. That is to say, if dual absorption peaks are expected to emerge for the composite with a thickness of 4.0 mm, the value of $|\mu_r\varepsilon_r|$ for 30 vol% composite should be improved at 0.1–18 GHz. Likely, this also is the reason why both the 10 vol% and 20 vol% filler composites under perfect impedance matching in Fig. 6 possess dual absorption peaks.

To discuss the EM wave absorbing mechanism, the minimum reflectivity for 30 vol% sample is small than the other volume concentration at perfect matching point in Fig. 6, which demonstrates the influence of interface reflection should not be neglected. Hence, the main absorbing mechanism for FeCrMoNiPBCSi amorphous powders/Silicone composite can be explained by the quarter-wavelength interface reflection and magnetic loss.

4. Conclusions

In this paper, the $Fe_{63}Cr_8Mo_{3.5}Ni_5P_{10}B_4C_4Si_{2.5}$ amorphous powder with high resistivity was chosen to prepare amorphous-filler composite. This alloy system is prone to achieve prominent impedance matching and strong EM wave attenuation with appropriate ratio of $\sqrt{\mu_r/\varepsilon_r}$. The 30 vol% filler composite reached reflection loss of −60.3 dB at 7.08 GHz with a perfect matching thickness of 3.55 mm, and dual absorption peaks were obtained at finite thickness beyond 4.01 mm, which facilitates broadening the absorbing bandwidth. The main absorbing mechanism can be explained by the quarter-wavelength interface reflection and magnetic loss.

Acknowledgments

This work was supported by the National Natural Science Foundation of China (Grant No. 51301189), Zhejiang Province Public Technology Research and Industrial Projects (Grant No. 2015C31043), Ningbo International Cooperation Projects (Grant No. 2015D10022) and Equipment Project for Research of the Chinese Academy of Sciences (Grant No. yz201434).

References

[1] E.F. Knott, J.F. Shaeffer, M.T. Tuley, Radar Cross Section, second ed., 2004. Boston.
[2] K.J. Vinoy, R.M. Jha, Radar Absorbing Materials: from Theory to Design and Characterization, 1996. Boston.
[3] Y.Y. Gu, X.Y. Qiu, Q.M. Hu, Y. Xue, Development of electromagnetic shielding material, Mater. Rev. 19 (2005) 53–56.
[4] W.J. Xu, D.G. Guang, G.L. Xu, Y. Sun, T. Chen, M.N. Zhao, C.M. Sun, Research progress and prospects of electromagnetic shielding materials, Saf. EMC 2 (2014) 57–60.
[5] Z.Z. Wang, P.H. Lin, W.C. Huang, S.K. Pan, Y. Liu, L. Wang, Effect of Ni content on microwave absorbing properties of MnAl powder, J. Magn. Magn. Mater 413 (2016) 9–13.
[6] R.B. Yang, W.F. Liang, C.H. Wu, C.C. Chen, Synthesis and microwave absorbing characteristics of functionally graded carbonyl iron/polyurethane composites, AIP Adv. 6 (2016) 055910.
[7] H. Yang, T. Ye, Y. Lin, M. Liu, Excellent microwave absorption property of ternary composite: polyaniline-$BaFe_{12}O_{19}$-$CoFe_2O_4$ powders, J. Alloy. Compd. 653 (2015) 135–139.
[8] X.L. Zheng, J. Feng, F.Z. Pu, Y.Y. Lan, Y. Zong, X.H. Li, H.J. Wu, Amorphous Fe_xB_{100-x} nanostructures: facile synthesis, magnetic properties and their applications as enhanced microwave absorbers at S- and C-bands, Adv. Powder Technol. 27 (2016) 704–710.
[9] M.G. Han, D.F. Liang, L.J. Deng, Fabrication and electromagnetic wave absorption properties of amorphous $Fe_{79}Si_{16}B_5$ microwires, Appl. Phys. Lett. 99 (2011) 082503.
[10] X.D. Wang, J.S. Liu, F.X. Qin, H. Wang, D.W. Xing, J.F. Sun, Microwave absorption properties of FeSiBNbCu glass-covered amorphous wires, T. Nonferr. Metal. Soc. 24 (2014) 2574–2580.
[11] Z.H. Zhang, C.D. Wang, Y.H. Zhang, J.X. Xie, Microwave absorbing properties of composites filled with glass-coated $Fe_{69}Co_{10}Si_8B_{13}$, amorphous microwire, Mater. Sci. Eng. B 175 (2010) 233–237.
[12] Y.J. Di, J.J. Jiang, G. Du, B. Tian, S.W. Bie, H.H. He, Magnetic and microwave properties of glass-coated amorphous ferromagnetic microwires, T. Nonferr. Metal. Soc. 17 (2007) 1352–1357.
[13] F.X. Qin, H.X. Peng, Ferromagnetic microwires enabled multifunctional composite materials, Prog. Mater. Sci. 58 (2010) 183–259.
[14] M.C. Elboubakraoui, N. Jebbor, B. Seddik, J. Foshi, Dielectric, magnetic and microwave absorbing properties of structural composites containing glass-coated amorphous microwires at X-band frequencies, Am. J. Mater. Sci. 6 (2016) 67–72.
[15] H. Matsumoto, A. Urata, Y. Yamada, A. Makino, To enhance the efficiency of a power supply circuit by the use of Fe-P-B-Nb-type ultralow loss glassy metal core, J. Appl. Phys. 105 (2009) 07A317.
[16] X.Y. Wang, C.W. Lu, F. Guo, Z.C. Lu, D.R. Li, S.X. Zhou, New Fe-based amorphous compound powder cores with superior DC-bias properties and low loss characteristics, J. Magn. Magn. Mater 24 (2012) 2727–2730.
[17] Y.Q. Dong, Q.K. Man, Z.D. Zhang, B.L. Shen, The soft magnetic properties of ring-shaped $(Co_{0.6}Fe_{0.3}Ni_{0.1})_{68}(B_{0.811}Si_{0.189})_{27}Nb_5$ bulk metallic glasses, J. Appl. Phys. 113 (2013) 17A336.
[18] V.A. Zhuravlev, V.I. Suslyaev, E.Y. Korovin, K.V. Dorozhkin, Electromagnetic waves absorbing characteristics of composite material containing carbonyl iron particles, Mater. Sci. Appl. 5 (2014) 803–811.
[19] J.R. Liu, M. Itoh, K. Machida, Electromagnetic wave absorption properties of α-$Fe/Fe_3B/Y_2O_3$ nanocomposites in gigahertz range, Appl. Phys. Lett. 83 (2003) 4017–4019.
[20] B.C. Wang, J.Q. Wei, Y. Yang, T. Wang, F.S. Li, Investigation on peak frequency of the microwave absorption for carbonyl iron/epoxy resin composite, J. Magn. Magn. Mater 323 (2011) 1101–1103.
[21] I. Kong, S.H. Ahmad, M.H. Abdullah, D. Hui, A.N. Yusoff, D. Puryanti, Magnetic and microwave absorbing properties of magnetite–thermoplastic natural rubber nanocomposites, J. Magn. Magn. Mater 322 (2010) 3401–3409.
[22] T. Inui, K. Konishi, K. Oda, Fabrications of broad-band rf-absorber composed of planar hexagonal ferrites, IEEE Int. (1999) 3148–3150.
[23] Z.W. Li, Z.H. Yang, The studies of high-frequency magnetic properties and absorption characteristics for amorphous-filler composites, J. Magn. Magn. Mater 391 (2015) 172–178.
[24] Z.W. Li, G.Q. Lin, L.B. Kong, Microwave reflection characteristics of Co_2Z Barium ferrite composites with various volume concentration, IEEE Trans. Magn. 44 (2008) 2255–2261.
[25] B.C. Wang, J.Q. Wei, L. Qiao, T. Wang, F.S. Li, Influence of the interface reflections on the microwave reflection loss for carbonyl iron/paraffin composite backed by a perfect conduction plate, J. Magn. Magn. Mater 324 (2012) 761–765.
[26] A. Berthault, D. Rousselle, G. Zerah, Magnetic properties of permalloy microparticles, J. Magn. Magn. Mater 112 (1992) 477–480.